A Generalized Enhancement Framework for Hazy Images With Complex Illumination

Zetian Mi, Yuanyuan Li, Jie Jin, Zheng Liang, and Xianping Fu

Abstract—**Images captured under low-light conditions are generally characterized by poor illumination, low contrast, and nonignorable large amount of noise. In order to improve the visibility in weak illumination scenes, multiple artificial light sources are used, which leads to severe uneven illumination of the scene. The main challenges of dehazing images with complex illumination are to suppress the boosting of unsightly noise when enhancing contrast and avoid overenhancement in bright glow regions. To circumvent problems above, this letter proposes a generalized enhancement framework, which works well not only in uniform light conditions but also in strongly nonuniform illumination low-light scenes. To achieve this, we first decompose the input hazy image into a structure layer containing low-frequency illumination variance and a texture layer containing large amount of high-frequency details. Sequentially, benefit from two derived masks that are intrinsically similar to weight maps, the proposed framework can perform regional adaptive brightness adjustment on the structure layer according to the distribution of light in the input image. Meanwhile, regions of effective details in the texture layer are assigned higher weights, while regions that belong to noise are suppressed. Finally, adding the enhanced texture layer back to the brightened structure layer, visually appealing results are generated. Experimental results on various scenarios demonstrate the superiority of the proposed framework over state-of-the-art methods in terms of both qualitative and quantitative.**

Index Terms—**Complex illumination, generalized enhancement model, image dehazing, low-light scenes.**

I. Introduction

As common weather phenomenon, haze and fog have brought serious negative influence to many vision-based techniques, such as tracking, video surveillance, and remote sensing missions [1]–[3], as shown in Fig. 1(a). When it comes to nighttime or deep sea, the problem becomes worse. Hazy images captured under low-light conditions are often characterized by poor illumination, low contrast, and obvious noise. Meanwhile, multiple artificial light sources cause a strong nonuniform illumination of the scene. These combined challenges make state-of-the-art dehazing techniques suffering from important limitations, say relatively bright regions and large amount of noise will be obviously overenhanced and wash out corresponding details.

(a)

(b)

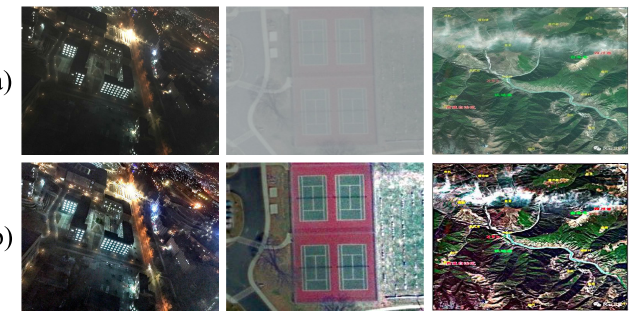

Fig. 1. Application of the proposed framework in dehazing remote sensing images with complex illumination. (a) Input remote sensing images. (b) Results generated by the proposed method.

Acquiring high-quality images is urgently demanded. Numerous dehazing methods have been proposed to improve the visibility of hazy scenes from the single image. The majority of pioneering works tackle this issue by inferencing the image degradation model, which is an ill-posed problem. Strong prior knowledge or assumptions are needed to estimate parameters, particularly the transmission and the atmospheric light. Generally, atmospheric light in daytime hazy image is considered to be the brightest region in the background. However, due to the nonuniform illumination in low-light conditions, multiple light sources seriously affect the estimation accuracy of the atmospheric light. As a result, although approaches based on dark channel prior (DCP) [4] and its variants [5]–[7], methods based on haze-line prior [8], [9], and so on have made remarkable successes, their effectiveness has been extensively demonstrated only on daytime dehazing, which is significantly unsatisfied in low-light hazy scenes.

To handle with the challenging issue, several researchers have paid attention to address the nighttime dehazing problem. Pei and Lee [10] first applied a color transfer function to reduce the color cast of the nighttime hazy image, before dehazing based on DCP. However, due to the changing of the original color distribution, unrealistic results with color artifacts tend to be generated. Similarly, Zhang *et al.* [11] performed color correction and estimated the nonuniform incident illumination before the DCP-based dehazing. However, the light compensation will affect the effectiveness of the subsequent color correction. Assuming that the local maximum

Manuscript received January 29, 2021; revised April 4, 2021; accepted May 9, 2021. This work was supported in part by the National Natural Science Foundation of China under Grant 61802043, in part by the Liaoning Revitalization Talents Program under Grant XLYC1908007, in part by the Foundation of Liaoning Key Research and Development Program under Grant 201801728, in part by the Fundamental Research Funds for the Central Universities under Grant 3132020215, and in part by the Dalian Science and Technology Innovation Fund under Grant 2018J12GX037 and Grant 2019J11CY001. *(Corresponding author: Zheng Liang.)*

Zetian Mi, Yuanyuan Li, Jie Jin, and Zheng Liang are with the School of Information Science and Technology, Dalian Maritime University, Dalian 116026, China (e-mail: mizetian@dlmu.edu.cn; lyy39906@163.com; jjie@dlmu.edu.cn; zliang@dlmu.edu.cn).

Xianping Fu is with the School of Information Science and Technology, Dalian Maritime University, Dalian 116026, China, and also with the Peng Cheng Laboratory, Shenzhen 518000, China (e-mail: fxp@dlmu.edu.cn).

Color versions of one or more figures in this letter are available at https://doi.org/10.1109/LGRS.2021.3079456.

Digital Object Identifier 10.1109/LGRS.2021.3079456

intensity is mainly contributed by the ambient illumination, the maximum reflectance prior (MRP) that is specific to nighttime is proposed by Zhang *et al.* [12]. By modeling the nighttime hazy image with uneven illumination as a linear superposition of the low-light background and glow effect, Li *et al.* [13] proposed a layer separation strategy to remove the glow of light sources. Finally, a DCP-based dehazing operation is followed to further improve the visibility. As observed, backgrounds recovered by this method tend to be too dark. Unfortunately, all methods above are limited to dealing with nighttime conditions. In order to estimate the atmospheric light more accurate and suitable for both daytime and nighttime dehazing, an effective fusion-based technique using the local airlight estimation is introduced by Ancuti *et al.* [14]. However, manual selection of patch sizes is inefficient, and when the lighting condition is very poor, this technique cannot work very well.

Inspired by the remarkable success achieved by deep learning-based computer vision tasks, many supervised learning-based methods for daytime dehazing [15], [16] are proposed. However, it is practically impossible to simultaneously obtain a low-light image with complex illumination and its corresponding ground truth. Lacking of sufficient large-scale dataset leads to largely unsatisfactory of deep learning-based methods. Although several nighttime hazy image synthetic methods [12], [17] are introduced, there still exists a gap between synthetic and real-world weak illumination images with complex lighting conditions.

To overcome the limitations faced by existing dehazing methods, a generalized enhancement framework is proposed in this letter. It can comprehensively address the challenging problems of hazy images with complex illumination. The main contributions are summarized as follows.

1) Dislike the most previous dehazing methods that are limited to specific lighting conditions, the proposed framework has universal applicability to enhance images captured under complex lighting scenario.
2) We introduce two masks that are intrinsically similar to weight maps in the generalized framework. These two masks reveal the distribution of illumination and texture in the input image, respectively, which subsequently determines the corresponding magnitude of enhancement. This strategy makes the proposed method completely regional adaptive.
3) A novel gamma correction approach is proposed. With the estimated lighting mask, this method can effectively improve the brightness of dark regions while suppressing the overenhancement of bright areas.

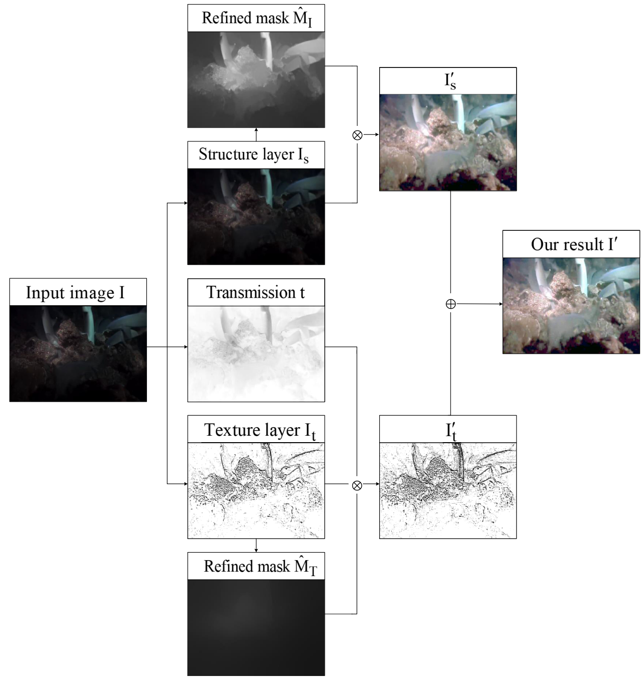

Fig. 2. Flowchart of the proposed framework. (Detail layers are reversed in order to facilitate the display.)

II. Proposed Method

Removing haze and adjusting the illumination are crucial for improving the visibility of low-light hazy images, which, however, is very challenging due to complex lighting conditions and easily amplified noise. To this end, a generalized enhancement framework for hazy images with complex illumination is proposed. The flowchart of the framework is shown in Fig. 2.

A. Structure-Texture Decomposition

Since hazy images taken under weak illumination often suffer from three kinds of degradation: complex distribution of illumination, low contrast, and nonignorable amount of noise, the image decomposition strategy is adopted to separate the low-frequency illumination and high-frequency textures including noise into corresponding layers, say structure and texture layers.

To make the problem simple, an edge-preserving filter is used to smooth the input image, whose result is regarded as the structure layer I_s. While the residual component I_t is obtained by subtracting the input image I with its smoothed version I_s. In our experiments, the guided filter [18] is adopted in view of its high efficiency and robustness. Therefore, I_s is piecewise smooth, which contains the illumination variance, while the majority of details and noise are captured in I_t.

Sequentially, adjusting illumination on the structure layer and enhancing contrast while suppressing noise on the texture layer separately, visually appealing results without unsightly noise can be generated.

B. Illumination Adjustment

Globally adjusting illumination over the entire image generally works well on pure low-light scenes, but it is not necessarily effective for low-light scenes with artificial light. To address this limitation, we propose a mask named M_I to reveal the illumination distribution of the input image. Formally, M_I is defined to be

$$M_I = \begin{cases} 1, & \text{mean}(I^c(x, y)) > \text{mean}(I_s) \\ 0, & \text{otherwise} \end{cases} \tag{1}$$

in which $c \in \{r, g, b\}$ is the color channel and (x, y) is the coordinate of the pixel. To avoid artifacts, the mask is then refined with the guided filter [18] and denoted as $\hat{M}_I$. Accordingly, $\hat{M}_I$ can indicate the light source locations and suppress the overadjustment of the illumination in these regions.

Hereafter, a new gamma correction strategy is proposed to adaptively adjust the illumination of I_s according to the distribution of light

$$\begin{aligned} \text{gamma} &= \alpha^{\frac{\hat{M}_I - \text{mean}(\hat{M}_I)}{\max(\hat{M}_I) - \min(\hat{M}_I)}} \\ \text{gamma}' &= \|1 - \beta * \text{gamma}\| \\ I_s' &= I_s^{\text{gamma}'} \end{aligned} \tag{2}$$

where α and β are two constant parameters. In order to significantly improve the brightness of dark regions while suppressing overenhancement of bright areas, $gamma'$ is constrained to $(0, 1)$. β is a constant that controls the strength of the amplification of illumination and manually set to 1.5 in our experiments. After deduction, α lies in $(0.75, 1) \cup (1, 1.33)$. Quantitative statistics on a large amount of experiments demonstrate that $\alpha = 1.2$ obtains the best performance.

C. Contrast Enhancement

1) Estimation of the Detail Mask: To avoid the unintentional boosting of unsightly noise when enhancing the contrast, a mask M_T is utilized to separate the texture layer $\boldsymbol{I}_t$ into detail and noise regions. Subsequently, noise can be suppressed as an integral part of the contrast enhancement procedure. Similar to [19] and [20], the discrete cosine transform (DCT) is applied to each 8×8 blocks in $\boldsymbol{I}_t$. DCT coefficients of each block is denoted as B. The likelihood indicating whether the block is detail or not is expressed as

$$\delta = \sum_{x,y} B_{x,y}^2 - B_{1,1}^2 - B_{1,2}^2 - B_{2,1}^2 \tag{3}$$

where x and y are coordinates. Since stronger high-frequency DCT coefficient means more details, M_T of this block is set to 1 when $\delta > threshold$ and to 0 otherwise. As recommended, $threshold$ is set to 0.1 in our experiments. Considering that M_T is a coarse version, we also utilize the guided filter [18] to refine M_T, thus obtaining $\hat{M}_T$.

2) Estimation of the Enhancement Factor: As described in the well-known image hazing model [4], the transmission is directly related to the degradation magnitude of the hazy image. Therefore, the reciprocal of the transmission is utilized to measure the magnitude of enhancement, which can achieve a physical sound performance. Following [21], t can be computed by adopting the fast transmission estimation method. Having created the mask indicating the regions of scene details, we now try to greatly enhance the effective details while suppressing the amplification of tiny details, including noise. To achieve this goal, a tanh function is introduced to stretch $\hat{M}_T$ to properly scale the textures. Hence, the contrast enhancement factor is defined as

$$\tau = \frac{\gamma \tanh(\hat{M}_T)}{t} \tag{4}$$

where $\tanh(x) = (e^x - e^{-x}/e^x + e^{-x})$ is the hyperbolic tangent function, γ is a constant parameter that controls the sigmoid curve, and t is the transmission. In general, setting γ around 2.5 results in visually pleasant outputs.

Finally, the enhanced image I' is recovered by

$$I' = I_s' + I_t', \text{ where } I_t' = \tau I_t \tag{5}$$

in which I_s' and I_t' are the reconstructed structure layer and texture layer, respectively, τ is the contrast enhancement factor computed in (4), and I_t is the texture layer. Namely, τI_t is the contrast recovered texture layer.

(a)
(b)
(c)

Fig. 3. Comparisons on enhancing pure low-light images. (a)–(c) Three raw pure low-light images and the corresponding results generated by different methods.

III. Experimental Results

To demonstrate the effectiveness of the proposed method, comparisons are carried out against several state-of-the-art low-light enhancement and dehazing methods on various scenarios with complex distribution of illumination: pure low-light scenes, real nighttime scenes with nonuniform illumination, underwater scenes, and daytime remote sensing hazy images, both qualitatively and quantitatively. For subjective evaluation, we test our approach on three datasets: low-light dataset (LOL) [22] which contains 485 low/normal-light image pairs, real-world nighttime hazy images (NHRW) [17] which consists of 150 NHRW, and underwater image enhancement benchmark (UIEB) [23] which includes 890 real-world underwater images with their corresponding references and 60 challenging images without reference. For quantitative evaluation, full-reference evaluation metrics peak signal-to-noise ratio (PSNR) and structural similarity index (SSIM) are used. For both, the larger the metrics, the better the quality.

All the experiments are performed on a PC with Intel i7-8700K at 3.7-GHz CPU with 32-GB RAM. The entire process for an image (approximately 1024×768 in size) using our unoptimized MATLAB implementation takes about 57 s with the main bottleneck being the overlapping sliding window-based estimation of M_T, whose computational complexity is $O(n^2)$ and taking about 55.58 s.

In Fig. 3, comparisons with several representative low-light enhancement techniques, including multiscale retinex (MSR), low-light image enhancement via illumination map estimation (LIME) [24], and structure-revealing (SR) [25], and nighttime dehazing methods, including Zhang *et al.* [11], MRP [12], and Li *et al.* [13] when handling pure low-light scenes, are presented. It can be easily observed that methods of Li *et al.* [13] and MRP [12] suffer from important limitations, where assumptions and prior they relied on generally fail. Although it achieves excellent performance in amplifying the brightness, the MSR method tends to significantly boost the unsightly noise. Results generated by LIME [24] and SR [25] show different degrees of oversaturation and oversmoothing. Zhang's method [11] can effectively improve the brightness and contrast, but unnatural artifacts tend to be introduced in smooth regions. By contrast, the proposed method shows excellent performance in terms of both the brightness adjustment and contrast enhancement.

Due to multiple light sources, real-world nighttime images are generally characterized by nonuniform illumination, which makes the dehazing task more challenging, thereby degrading the performance of daytime dehazing techniques. To illustrate the advantages achieved by the proposed framework, comparisons against two representative daytime dehazing

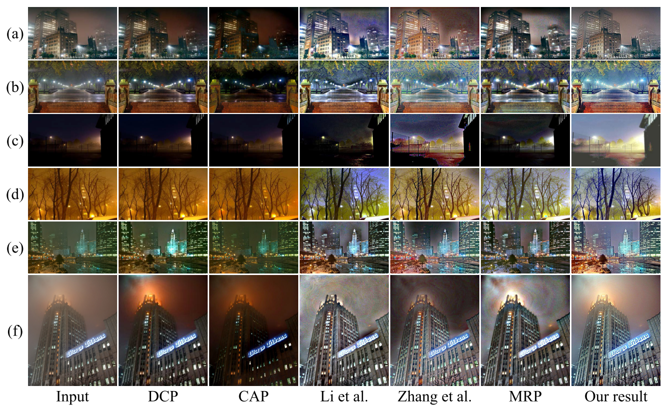

Fig. 4. Comparisons on dehazing NHRW with nonuniform illumination. (a)–(f) Six raw real-world nighttime hazy images and the corresponding results generated by different methods.

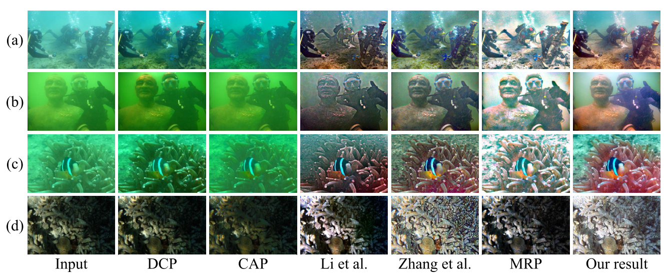

Fig. 5. Comparisons on dehazing underwater images with weak illumination. (a)–(d) Four raw underwater images from UIEB [23] testing set and the corresponding results generated by different methods.

techniques, including DCP [4] and color attenuation prior (CAP) [26], and three abovementioned specialized nighttime dehazing methods [11]–[13] are presented in Fig. 4. As can be seen from the results, daytime dehazing techniques perform poorly for the task of nighttime dehazing. They have very little effect on brightness improvement and contrast enhancement. On the contrary, the specialized nighttime dehazing methods generate visually more compelling results. From Fig. 4(a), (b), (e), and (f), we can see that the method of Li *et al.* [13] removes the majority of glow effect and generates clear images. However, significant artifacts around light sources are introduced and limitations appear in Fig. 4(c). Zhang' approach [11] performs better in brightness adjustment but leads to prominently visible noise. In addition, its result presented in Fig. 4(c) is severely unsatisfactory due to the significant manual processing trace. The MRP method [12] tends to generate less contrasted results than the proposed method, which can be seen easily from the sixth column of Fig. 4(a), (b), (d), and (f), especially in light source regions of Fig. 4(a). In addition, obvious artifacts are produced in smooth areas [e.g., sky regions in Fig. 4(a), (c), and (f)]. As expected, due to the natural appearance and better details, the proposed approach achieves almost the best visual quality among all.

Due to the severe absorption and scattering of light, underwater images are usually captured in low-light conditions, whose restoration is also a challenging task to be solved urgently. To further demonstrate the effectiveness of the proposed framework, comparisons against these dehazing techniques in dealing with underwater scenes are presented in Figs. 5 and 6. As shown in Fig. 5, the results generated by CAP [26] are almost the same as the original input images. The DCP method [4] does not play a positive role in brightness

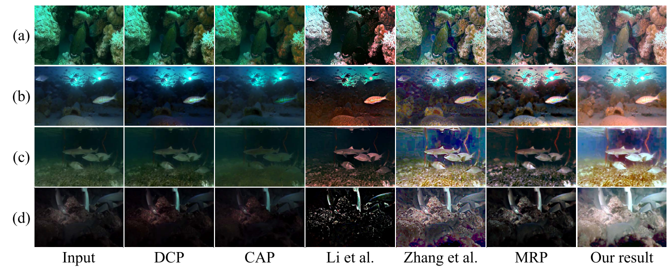

Fig. 6. Comparisons on dehazing challenging underwater images with complex illumination. (a)–(d) Four raw underwater images from UIEB [23] challenging set and the corresponding results generated by different methods.

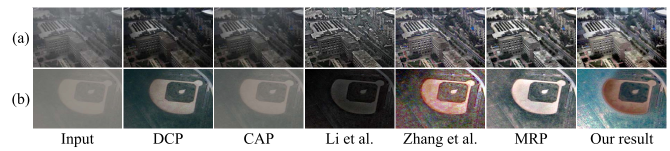

Fig. 7. Comparisons on dehazing daytime remote sensing images. (a) and (b) Two raw remote sensing images and the corresponding results generated by different methods.

TABLE I

PSNR AND SSIM VALUES OF DIFFERENT METHODS IN FIG. 3

		MSR	LIME [24]	SR [25]	Li et el. [13]	Zhang et al. [11]	MRP [12]	Our result
(a)	PSNR	18.81	11.87	14.48	9.77	14.04	9.43	**21.04**
	SSIM	0.81	0.70	0.82	0.46	0.54	0.45	**0.86**
(b)	PSNR	**23.54**	10.12	10.53	5.84	14.22	5.79	19.17
	SSIM	0.63	0.44	0.59	0.17	0.34	0.16	**0.68**
(c)	PSNR	11.88	22.71	**28.77**	16.00	16.17	16.68	13.69
	SSIM	0.72	0.83	**0.90**	0.72	0.59	0.73	0.76
aver	PSNR	**16.22**	15.30	13.86	9.04	14.62	8.90	15.70
	SSIM	0.52	0.44	**0.62**	0.34	0.31	0.35	0.59

adjustment and color correction, but only slightly enhances the contrast. By contrast, nighttime dehazing methods are also competitive for underwater image enhancement. Among these methods, Li's method [13] tends to darken the image and generates unnatural reddish results. MRP [12] achieves the worst results in terms of visual effects. Specifically, in the sixth column of Fig. 5(a)–(c), inaccurate color cast estimation leads to whitish results. On the contrary, the proposed method performs comparable to Zhang's method [11] but is superior to it in terms of visibility improvement and noise suppression.

In Fig. 6, comparisons with the abovementioned methods are carried out on challenging underwater images in the UIEB [23] dataset. Generally, these images are characterized by relatively weak illumination and artificial light, which makes the majority of physical-model-based methods failed and results in visually unpleasing restoration outputs. As can be observed, daytime dehazing methods as DCP [4] and CAP [26] still perform poorly in these scenes. Results generated by Li *et al.* [13] and MRP [12] are also unsatisfactory, while in the fifth column of Fig. 6, prominently artifacts are tend to be introduced in results generated by Zhang *et al.*'s method [11].

In Fig. 7, we further present the performance of the proposed framework in dehazing daytime remote sensing images. As can be observed, nighttime dehazing methods, such as Zhang *et al.*'s [11], MRP [12], and our approach, show better stability and applicability in these scenarios. However, Zhang's method tends to generate results with color artifacts and amplified noise, while in these environments without complicated lighting, our method and MRP [12] are comparable to each other.

Furthermore, in order to quantitatively evaluate the performance of the proposed method, full-reference evaluation using two well-known metrics: PSNR and SSIM are shown

TABLE II
PSNR AND SSIM VALUES OF DIFFERENT METHODS IN FIG. 5

		DCP [4]	CAP [26]	Li et el. [13]	Zhang et al. [11]	MRP [12]	Our result
(a)	PSNR	18.80	16.01	17.37	18.65	16.46	**23.49**
	SSIM	**0.78**	0.66	0.71	0.75	0.76	0.77
(b)	PSNR	16.05	17.82	15.79	18.44	16.03	**24.28**
	SSIM	0.78	0.78	0.84	0.88	0.74	**0.94**
(c)	PSNR	19.78	18.31	16.26	17.44	15.47	**20.53**
	SSIM	**0.94**	0.87	0.84	0.87	0.76	0.88
(d)	PSNR	11.74	10.52	15.36	19.01	13.15	**21.76**
	SSIM	0.59	0.49	0.73	0.78	0.68	**0.82**
aver	PSNR	**20.52**	16.69	18.73	19.18	19.20	20.03
	SSIM	**0.88**	0.76	0.82	0.84	0.81	0.87

in Tables I and II. Since we do not have all the ground-truth images, quantitative evaluation is only performed on the entire LOL and UIEB datasets. As shown in Table I, Li's method [13] and MRP [12] achieve equally the worst scores for all the metrics on Fig. 3(a) and (b) and average values over the LOL dataset, which is consistent with the subjective performance. Although they obtain higher PSNR values on Fig. 3(c), the corresponding subjective results are not satisfactory. It is interesting that MSR achieves the highest PSNR score. However, as can be seen from Fig. 3(b), noise becomes significantly visible in its corresponding result. Though results produced by LIME [24] and SR [25] achieve higher scores on both the PSNR and SSIM metrics than the proposed method in Fig. 3(c), they are visually inferior in actual.

Consistent with the subjective performance, the proposed approach stands out as the competitive best performer in Table II, which indicates the robustness of our method. However, the phenomenon that assessments are biased toward overenhancement results still exists. Daytime dehazing methods as DCP [4] and CAP [26] could preserve image structures to some extent. However, since they are not designed for underwater scenes, color deviation is maintained and details are not enhanced well.

IV. CONCLUSION

In this letter, a generalized enhancement framework for hazy images with complex illumination is introduced, which is proved to be suitable for hazy scenes with various distributions of illumination. To compensate for the brightness and contrast independently, we first separate the piecewise smooth variance of illumination into the structure layer and details into the texture layer. Then, two masks, indicating the distribution of light and effective detail regions, respectively, are derived. Benefit from these two masks that are similar to weight maps, the proposed framework can perform regional adaptive brightness adjustment and contrast enhancement. Finally, adding the proper scaled structure layer and texture layer together to generate visually appealing results. Both qualitative and quantitative comparisons illustrate that the proposed framework has superior robustness, accuracy, and flexibility for diverse scenes with complex distribution of light.

However, the proposed method is not without limitations. The computational efficiency makes it unsuitable for real-time applications, which needs to be further improved in future work.

REFERENCES

[1] S. Matteoli, G. Corsini, M. Diani, G. Cecchi, and G. Toci, "Automated underwater object recognition by means of fluorescence LiDAR," *IEEE Trans. Geosci. Remote Sens.*, vol. 53, no. 1, pp. 375–393, Jan. 2015.

[2] X. Liu, Z. Gao, and B. M. Chen, "MLFcGAN: Multilevel feature fusion-based conditional GAN for underwater image color correction," *IEEE Geosci. Remote Sens. Lett.*, vol. 17, no. 9, pp. 1488–1492, Sep. 2020.

[3] K. Jiang, Z. Wang, P. Yi, G. Wang, T. Lu, and J. Jiang, "Edge-enhanced GAN for remote sensing image superresolution," *IEEE Trans. Geosci. Remote Sens.*, vol. 57, no. 8, pp. 5799–5812, Aug. 2019.

[4] K. He, J. Sun, and X. Tang, "Single image haze removal using dark channel prior," *IEEE Trans. Pattern Anal. Mach. Intell.*, vol. 33, no. 12, pp. 2341–2353, Dec. 2011.

[5] Q. Wu, J. Zhang, W. Ren, W. Zuo, and X. Cao, "Accurate transmission estimation for removing haze and noise from a single image," *IEEE Trans. Image Process.*, vol. 29, pp. 2583–2597, Jan. 2020.

[6] W. Wang, X. Yuan, X. Wu, and Y. Dong, "An airlight estimation method for image dehazing based on gray projection," *Multimedia Tools Appl.*, vol. 79, nos. 37–38, pp. 27185–27203, Oct. 2020.

[7] W. Wang, X. Yuan, X. Wu, and Y. Liu, "Fast image dehazing method based on linear transformation," *IEEE Trans. Multimedia*, vol. 19, no. 6, pp. 1142–1155, Jun. 2017.

[8] R. Fattal, "Dehazing using color-lines," *ACM Trans. Graph.*, vol. 34, no. 1, pp. 1–14, Dec. 2014.

[9] D. Berman, T. Treibitz, and S. Avidan, "Single image dehazing using haze-lines," *IEEE Trans. Pattern Anal. Mach. Intell.*, vol. 42, no. 3, pp. 720–734, Mar. 2020.

[10] S.-C. Pei and T.-Y. Lee, "Nighttime haze removal using color transfer pre-processing and dark channel prior," in *Proc. 19th IEEE Int. Conf. Image Process.*, Sep. 2012, pp. 957–960.

[11] J. Zhang, Y. Cao, and Z. Wang, "Nighttime haze removal based on a new imaging model," in *Proc. IEEE Int. Conf. Image Process. (ICIP)*, Oct. 2014, pp. 4557–4561.

[12] J. Zhang, Y. Cao, S. Fang, Y. Kang, and C. W. Chen, "Fast haze removal for nighttime image using maximum reflectance prior," in *Proc. IEEE Conf. Comput. Vis. Pattern Recognit. (CVPR)*, Jul. 2017, pp. 7418–7426.

[13] Y. Li, R. T. Tan, and M. S. Brown, "Nighttime haze removal with glow and multiple light colors," in *Proc. IEEE Int. Conf. Comput. Vis. (ICCV)*, Dec. 2015, pp. 226–234.

[14] C. Ancuti, C. O. Ancuti, C. De Vleeschouwer, and A. C. Bovik, "Day and night-time dehazing by local airlight estimation," *IEEE Trans. Image Process.*, vol. 29, pp. 6264–6275, May 2020.

[15] B. Cai, X. Xu, K. Jia, C. Qing, and D. Tao, "DehazeNet: An end-to-end system for single image haze removal," *IEEE Trans. Image Process.*, vol. 25, no. 11, pp. 5187–5198, Nov. 2016.

[16] W. Ren, J. Pan, H. Zhang, X. Cao, and M.-H. Yang, "Single image dehazing via multi-scale convolutional neural networks with holistic edges," *Int. J. Comput. Vis.*, vol. 128, no. 1, pp. 240–259, Jan. 2020.

[17] J. Zhang, Y. Cao, Z.-J. Zha, and D. Tao, "Nighttime dehazing with a synthetic benchmark," in *Proc. 28th ACM Int. Conf. Multimedia*, Oct. 2020, pp. 2355–2363.

[18] K. He, J. Sun, and X. Tang, "Guided image filtering," *IEEE Trans. Pattern Anal. Mach. Intell.*, vol. 35, no. 6, pp. 1397–1409, Jun. 2013.

[19] Y. Li, F. Guo, R. T. Tan, and M. S. Brown, "A contrast enhancement framework with JPEG artifacts suppression," in *Proc. ECCV*, Sep. 2014, pp. 174–188.

[20] J. Yang, X. Wang, H. Yue, X. Fu, and C. Hou, "Underwater image enhancement based on structure-texture decomposition," in *Proc. IEEE Int. Conf. Image Process. (ICIP)*, Sep. 2017, pp. 1207–1211.

[21] J.-P. Tarel and N. Hautiere, "Fast visibility restoration from a single color or gray level image," in *Proc. IEEE 12th Int. Conf. Comput. Vis.*, Sep. 2009, pp. 2201–2208.

[22] C. Wei, W. Wang, W. Yang, and J. Liu, "Deep retinex decomposition for low-light enhancement," 2018, *arXiv:1808.04560*. [Online]. Available: https://arxiv.org/abs/1808.04560

[23] C. Li *et al.*, "An underwater image enhancement benchmark dataset and beyond," *IEEE Trans. Image Process.*, vol. 29, pp. 4376–4389, Feb. 2020.

[24] X. Guo, Y. Li, and H. Ling, "LIME: Low-light image enhancement via illumination map estimation," *IEEE Trans. Image Process.*, vol. 26, no. 2, pp. 982–993, Feb. 2017.

[25] M. Li, J. Liu, W. Yang, X. Sun, and Z. Guo, "Structure-revealing low-light image enhancement via robust retinex model," *IEEE Trans. Image Process.*, vol. 27, no. 6, pp. 2828–2841, Jun. 2018.

[26] Q. Zhu, J. Mai, and L. Shao, "A fast single image haze removal algorithm using color attenuation prior," *IEEE Trans. Image Process.*, vol. 24, no. 11, pp. 3522–3533, Nov. 2015.